

## Electronic Supplementary Information

### The conformational behavior of naproxen and flurbiprofen in solution

#### by NMR spectroscopy

**Maria Enrica Di Pietro<sup>a,\*</sup>, Christie Aroulanda<sup>b</sup>, Giorgio Celebre<sup>a</sup>, Denis Merlet<sup>b,\*</sup> and**

**Giuseppina De Luca<sup>a,\*</sup>**

<sup>a</sup> Lab. LXNMR\_S.C.An., Dipartimento di Chimica e Tecnologie Chimiche, Università della Calabria, via P. Bucci, 87036, Arcavacata di Rende (CS), Italy.

<sup>b</sup> Equipe de RMN en milieu orienté, ICMMO, UMR 8182 CNRS, Université Paris-Sud, 15 rue Georges Clemenceau, 91405, Orsay, France.

**Table 1.** Experimental  $^1\text{H}$  and  $^{13}\text{C}$  chemical shifts  $\delta_k$  of NAP and FLU determined by the NMR analysis in PBLG/THF- $d_8$ . Calibration is given from THF signal (at 1.72 ppm and 25.37 ppm, respectively).

NAP				FLU			
$k$	$\delta_k$ (ppm)	$k$	$\delta_k$ (ppm)	$k$	$\delta_k$ (ppm)	$k$	$\delta_k$ (ppm)
H <sub>2</sub>	3.79 ± 0.05	C <sub>1</sub>	175.8 ± 0.3	H <sub>2</sub>	3.76 ± 0.08	C <sub>1</sub>	175.2 ± 0.3
H <sub>3</sub>	1.51 ± 0.05	C <sub>2</sub>	46.0 ± 0.3	H <sub>3</sub>	1.50 ± 0.08	C <sub>2</sub>	45.6 ± 0.3
H <sub>5</sub>	7.42 ± 0.05	C <sub>3</sub>	19.2 ± 0.3	H <sub>5</sub>	7.21 ± 0.08	C <sub>3</sub>	19.1 ± 0.3
H <sub>6</sub>	7.68 ± 0.05	C <sub>4</sub>	137.6 ± 0.3	H <sub>8</sub>	7.46 ± 0.08	C <sub>4</sub>	144.5 ± 0.3
H <sub>8</sub>	7.17 ± 0.05	C <sub>5</sub>	127.2 ± 0.3	H <sub>9</sub>	7.33 ± 0.08	C <sub>5</sub>	116.1 ± 0.3
H <sub>10</sub>	7.09 ± 0.05	C <sub>6</sub>	127.7 ± 0.3	H <sub>11</sub> , H <sub>15</sub>	7.54 ± 0.08	C <sub>6</sub>	160.7 ± 0.3
H <sub>11</sub>	7.68 ± 0.05	C <sub>7</sub>	134.9 ± 0.3	H <sub>12</sub> , H <sub>14</sub>	7.49 ± 0.08	C <sub>7</sub>	128.5 ± 0.3
H <sub>13</sub>	7.69 ± 0.05	C <sub>8</sub>	106.3 ± 0.3	H <sub>13</sub>	7.41 ± 0.08	C <sub>8</sub>	131.5 ± 0.3
H <sub>14</sub>	3.85 ± 0.05	C <sub>9</sub>	158.8 ± 0.3			C <sub>9</sub>	124.7 ± 0.3
		C <sub>10</sub>	119.6 ± 0.3			C <sub>10</sub>	136.9 ± 0.3
		C <sub>11</sub>	129.9 ± 0.3			C <sub>11</sub> , C <sub>15</sub>	129.7 ± 0.3
		C <sub>12</sub>	130.1 ± 0.3			C <sub>12</sub> , C <sub>14</sub>	129.2 ± 0.3
		C <sub>13</sub>	126.7 ± 0.3			C <sub>13</sub>	128.5 ± 0.3
		C <sub>14</sub>	55.5 ± 0.3				

**Table 2.** Experimental scalar couplings  $J_{ij}^{obs}$  and total couplings  $T_{ij}^{obs}$  determined by the NMR analysis of NAP dissolved in THF-d<sub>8</sub> and PBLG/THF-d<sub>8</sub>. Errors are estimated from spectral resolution.

<i>i</i>	<i>j</i>	$J_{ij}^{obs}$ (Hz)	$T_{ij}^{obs}$ (Hz)	<i>i</i>	<i>j</i>	$J_{ij}^{obs}$ (Hz)	$T_{ij}^{obs}$ (Hz)
<i>C-H couplings</i>				<i>H-H couplings</i>			
C <sub>2</sub>	H <sub>2</sub>	129.7 ± 0.6	246.3 ± 0.6	H <sub>2</sub>	H <sub>3</sub>	7.2 ± 0.2	20.5 ± 0.8
C <sub>2</sub>	H <sub>5</sub>	3.4 ± 0.4	6.5 ± 0.6	H <sub>2</sub>	H <sub>5</sub>	0.0 ± 0.2	-6.8 ± 0.2
C <sub>3</sub>	H <sub>2</sub>	-4.2 ± 0.4	7.0 ± 0.6	H <sub>3</sub>	H <sub>3</sub>	-	-29.0 ± 0.8
C <sub>3</sub>	H <sub>3</sub>	128.4 ± 0.6	115.7 ± 0.6	H <sub>3</sub>	H <sub>5</sub>	0.0 ± 0.2	1.0 ± 0.2
C <sub>4</sub>	H <sub>2</sub>	-6.7 ± 0.4	-9.3 ± 0.8	H <sub>5</sub>	H <sub>6</sub>	8.5 ± 0.2	-35.7 ± 0.4
C <sub>4</sub>	H <sub>3</sub>	4.5 ± 0.6	4.4 ± 0.6	H <sub>5</sub>	H <sub>8</sub>	0.0 ± 0.2	-6.2 ± 0.4
C <sub>4</sub>	H <sub>5</sub>	0.0 ± 0.4	14.7 ± 0.8	H <sub>5</sub>	H <sub>14</sub>	0.0 ± 0.2	-2.0 ± 0.2
C <sub>5</sub>	H <sub>2</sub>	5.2 ± 0.4	3.0 ± 0.8	H <sub>6</sub>	H <sub>8</sub>	1.2 ± 0.2	-33.9 ± 0.4
C <sub>5</sub>	H <sub>5</sub>	156.9 ± 0.6	171.2 ± 0.8	H <sub>6</sub>	H <sub>10</sub>	0.0 ± 0.2	1.8 ± 0.4
C <sub>5</sub>	H <sub>13</sub>	7.8 ± 0.4	11.2 ± 0.6	H <sub>6</sub>	H <sub>11</sub>	0.0 ± 0.2	4.3 ± 0.4
C <sub>6</sub>	H <sub>6</sub>	157.7 ± 0.6	238.0 ± 0.6	H <sub>6</sub>	H <sub>13</sub>	0.9 ± 0.2	4.3 ± 0.4
C <sub>7</sub>	H <sub>5</sub>	8.2 ± 0.4	6.4 ± 0.8	H <sub>6</sub>	H <sub>14</sub>	0.0 ± 0.2	-4.1 ± 0.2
C <sub>8</sub>	H <sub>8</sub>	157.9 ± 0.6	233.1 ± 0.6	H <sub>8</sub>	H <sub>10</sub>	2.6 ± 0.2	9.5 ± 0.4
C <sub>8</sub>	H <sub>11</sub>	-1.3 ± 0.6	0.0 ± 0.6	H <sub>8</sub>	H <sub>11</sub>	0.7 ± 0.2	4.3 ± 0.4
C <sub>8</sub>	H <sub>14</sub>	0.0 ± 0.6	-4.4 ± 0.8	H <sub>8</sub>	H <sub>14</sub>	-0.3 ± 0.1	28.8 ± 0.4
C <sub>10</sub>	H <sub>8</sub>	5.7 ± 0.6	9.4 ± 0.6	H <sub>10</sub>	H <sub>11</sub>	8.9 ± 0.2	-39.8 ± 0.4
C <sub>10</sub>	H <sub>10</sub>	160.1 ± 0.6	176.0 ± 0.6	H <sub>11</sub>	H <sub>13</sub>	0.6 ± 0.2	-32.8 ± 0.4
C <sub>11</sub>	H <sub>8</sub>	0.0 ± 0.6	1.5 ± 0.6	H <sub>14</sub>	H <sub>14</sub>	-	-22.0 ± 0.4
C <sub>11</sub>	H <sub>11</sub>	159.2 ± 0.6	234.2 ± 0.8				
C <sub>11</sub>	H <sub>13</sub>	5.1 ± 0.6	-4.5 ± 0.6				
C <sub>13</sub>	H <sub>2</sub>	6.0 ± 0.4	0.0 ± 0.8				
C <sub>13</sub>	H <sub>5</sub>	6.2 ± 0.4	9.1 ± 0.8				
C <sub>13</sub>	H <sub>13</sub>	156.7 ± 0.6	232.6 ± 0.8				
C <sub>14</sub>	H <sub>8</sub>	0.0 ± 0.6	-6.8 ± 0.6				
C <sub>14</sub>	H <sub>14</sub>	143.6 ± 0.6	132.9 ± 0.6				

**Table 3.** Experimental scalar couplings  $J_{ij}^{obs}$  and total couplings  $T_{ij}^{obs}$  determined by the NMR analysis of FLU dissolved in THF-d<sub>8</sub> and PBLG/THF-d<sub>8</sub>. Errors are estimated from spectral resolution.

<i>i</i>	<i>j</i>	$J_{ij}^{obs}$ (Hz)	$T_{ij}^{obs}$ (Hz)	<i>i</i>	<i>j</i>	$J_{ij}^{obs}$ (Hz)	$T_{ij}^{obs}$ (Hz)
<i>C-H couplings</i>				<i>H-H couplings</i>			
C <sub>1</sub>	H <sub>2</sub>	-7.5 ± 0.3	-5.2 ± 0.6	H <sub>2</sub>	H <sub>3</sub>	7.2 ± 0.1	22.2 ± 0.2
C <sub>1</sub>	H <sub>3</sub>	4.7 ± 0.3	7.3 ± 0.7	H <sub>2</sub>	H <sub>5</sub>	-0.6 ± 0.1	-20.0 ± 0.3
C <sub>1</sub>	H <sub>5</sub>	-1.4 ± 0.5	-3.3 ± 0.8	H <sub>2</sub>	H <sub>8</sub>	0.0 ± 0.1	-3.0 ± 0.3
C <sub>2</sub>	H <sub>2</sub>	130.6 ± 0.3	223.2 ± 0.3	H <sub>2</sub>	H <sub>9</sub>	-0.8 ± 0.1	-12.1 ± 0.3
C <sub>2</sub>	H <sub>3</sub>	-4.2 ± 0.3	0.0 ± 0.6	H <sub>3</sub>	H <sub>3</sub>	-	-36.8 ± 0.2
C <sub>3</sub>	H <sub>2</sub>	-4.3 ± 0.3	6.2 ± 0.8	H <sub>3</sub>	H <sub>5</sub>	0.0 ± 0.1	-6.0 ± 0.3
C <sub>3</sub>	H <sub>3</sub>	128.8 ± 0.3	112.2 ± 0.3	<i>H-F couplings</i>			
C <sub>4</sub>	H <sub>2</sub>	-6.8 ± 0.4	-9.4 ± 0.7	H <sub>5</sub>	F <sub>6</sub>	12.0 ± 0.1	-24.0 ± 0.2
C <sub>4</sub>	H <sub>3</sub>	4.7 ± 0.4	4.7 ± 0.7	H <sub>8</sub>	F <sub>6</sub>	8.4 ± 0.1	12.3 ± 0.2
C <sub>5</sub>	H <sub>2</sub>	5.4 ± 0.3	2.0 ± 0.7	H <sub>11</sub>	F <sub>6</sub>	1.7 ± 0.1	-4.5 ± 0.2
C <sub>5</sub>	H <sub>3</sub>	0.0 ± 0.3	0.0 ± 0.6	H <sub>15</sub>	F <sub>6</sub>	1.7 ± 0.1	-4.5 ± 0.2
C <sub>5</sub>	H <sub>5</sub>	160.6 ± 0.3	215.2 ± 0.3	<i>C-F couplings</i>			
C <sub>5</sub>	H <sub>9</sub>	7.1 ± 0.3	9.2 ± 0.3	C <sub>2</sub>	F <sub>6</sub>	1.4 ± 0.3	0.0 ± 0.3
C <sub>8</sub>	H <sub>8</sub>	159.3 ± 0.3	208.5 ± 0.8	C <sub>4</sub>	F <sub>6</sub>	7.7 ± 0.3	6.4 ± 0.3
C <sub>9</sub>	H <sub>2</sub>	5.3 ± 0.3	2.0 ± 0.7	C <sub>5</sub>	F <sub>6</sub>	23.7 ± 0.3	15.6 ± 0.3
C <sub>9</sub>	H <sub>3</sub>	0.0 ± 0.3	0.0 ± 0.7	C <sub>6</sub>	F <sub>6</sub>	-247.0 ± 0.3	-239.0 ± 0.3
C <sub>9</sub>	H <sub>8</sub>	-1.3 ± 0.3	-10.2 ± 0.3	C <sub>7</sub>	F <sub>6</sub>	13.5 ± 0.3	20.7 ± 0.3
C <sub>9</sub>	H <sub>9</sub>	159.5 ± 0.3	169.0 ± 0.3	C <sub>8</sub>	F <sub>6</sub>	3.9 ± 0.3	5.6 ± 0.3
C <sub>11</sub>	H <sub>11</sub>	160.1 ± 0.3	207.0 ± 0.8	C <sub>9</sub>	F <sub>6</sub>	3.3 ± 0.3	3.4 ± 0.3
C <sub>15</sub>	H <sub>15</sub>	160.1 ± 0.3	207.0 ± 0.8	C <sub>11</sub>	F <sub>6</sub>	3.0 ± 0.3	2.4 ± 0.3
C <sub>12</sub>	H <sub>11</sub>	-1.4 ± 0.5	-12.4 ± 0.3	C <sub>15</sub>	F <sub>6</sub>	3.0 ± 0.3	2.4 ± 0.3
C <sub>14</sub>	H <sub>15</sub>	-1.4 ± 0.5	-12.4 ± 0.3				
C <sub>12</sub>	H <sub>12</sub>	160.7 ± 0.3	208.4 ± 0.8				
C <sub>14</sub>	H <sub>14</sub>	160.7 ± 0.3	208.4 ± 0.8				
C <sub>13</sub>	H <sub>13</sub>	160.7 ± 0.3	39.2 ± 0.8				

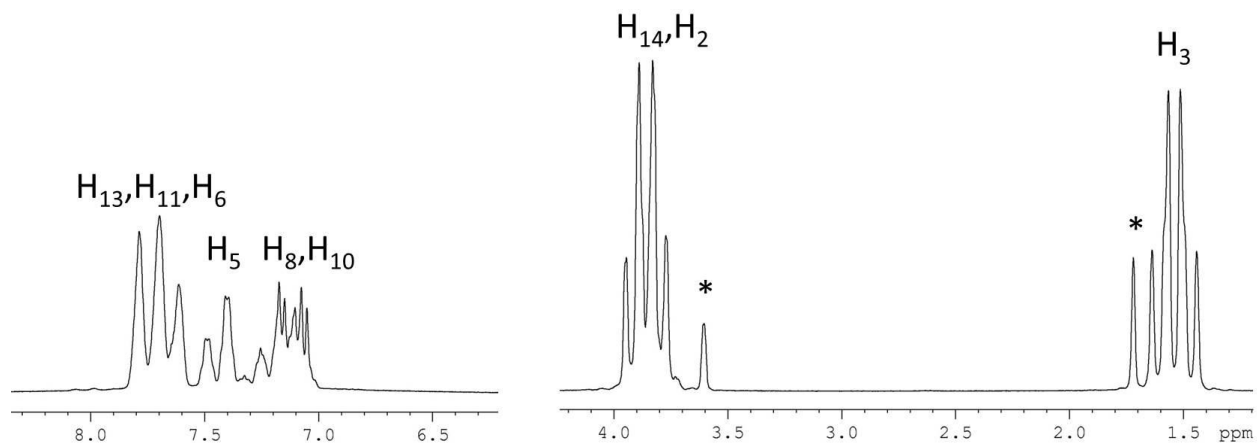


**Figure 1.** 1D  $^1\text{H}$  spectrum (Larmor frequency 400.13 MHz) recorded on *S*-naproxen in PBLG/THF- $d_8$  at 300 K. Solvent peaks are labeled with asterisks.

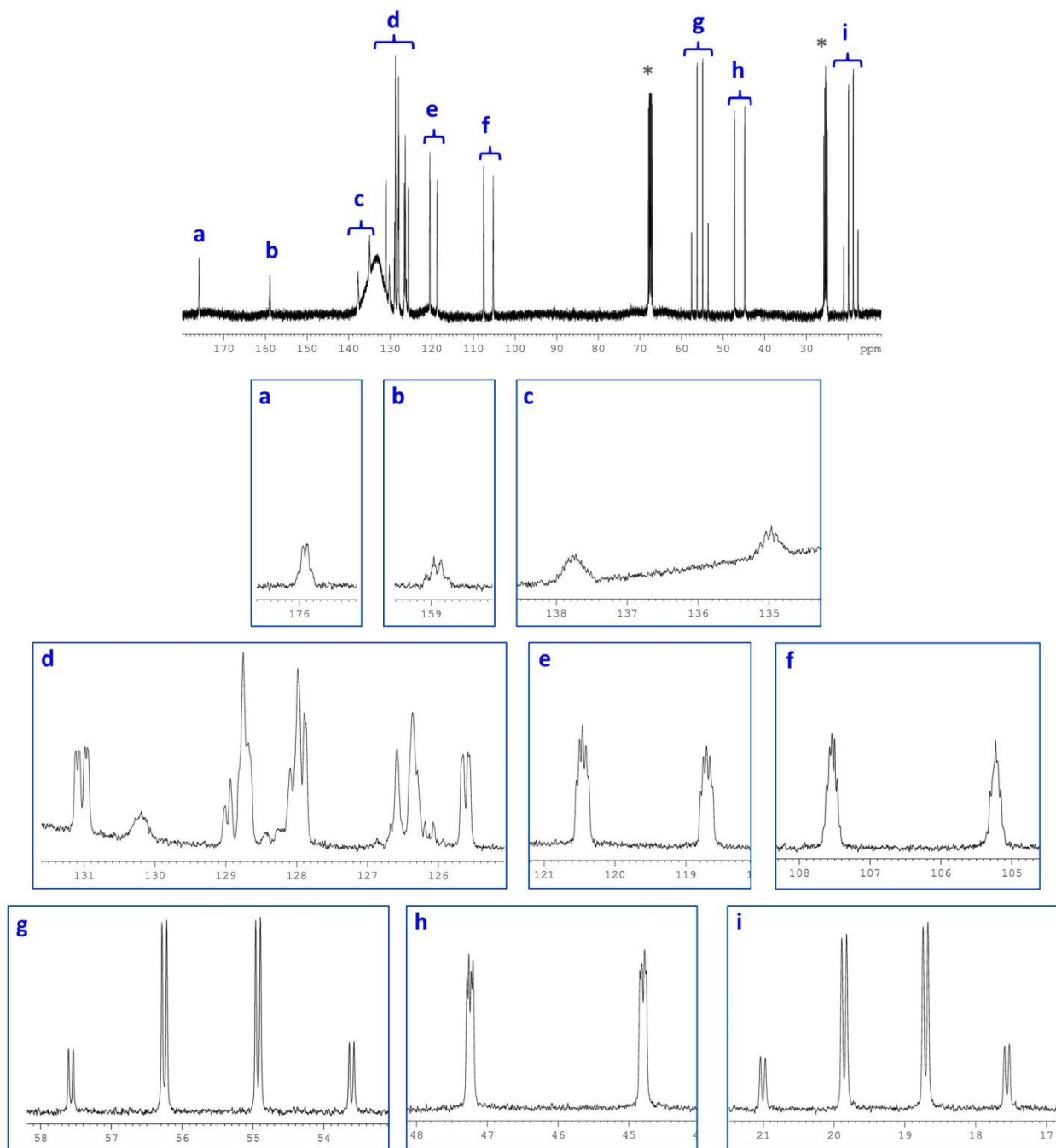


**Figure 2.** 1D  $^{13}\text{C}$  spectrum (Larmor frequency 100.61 MHz) recorded on S-naproxen in PBLG/THF- $\text{d}_8$  at 300 K. Solvent peaks are labeled with asterisks. Signals corresponding to each carbon atom are labeled with different letters: (a)  $\text{C}_1$ ; (b)  $\text{C}_9$ ; (c)  $\text{C}_4$ ,  $\text{C}_7$ ; (d)  $\text{C}_{12}$ ;  $\text{C}_{11}$ ;  $\text{C}_6$ ;  $\text{C}_5$ ;  $\text{C}_{13}$ ; (e)  $\text{C}_{10}$ ; (f)  $\text{C}_8$ ; (g)  $\text{C}_{12}$ ; (h)  $\text{C}_2$ ; (i)  $\text{C}_3$ . The spectrum was recorded by using 32768 points and 8192 scans and processed using zero-filling up to 65536 points.

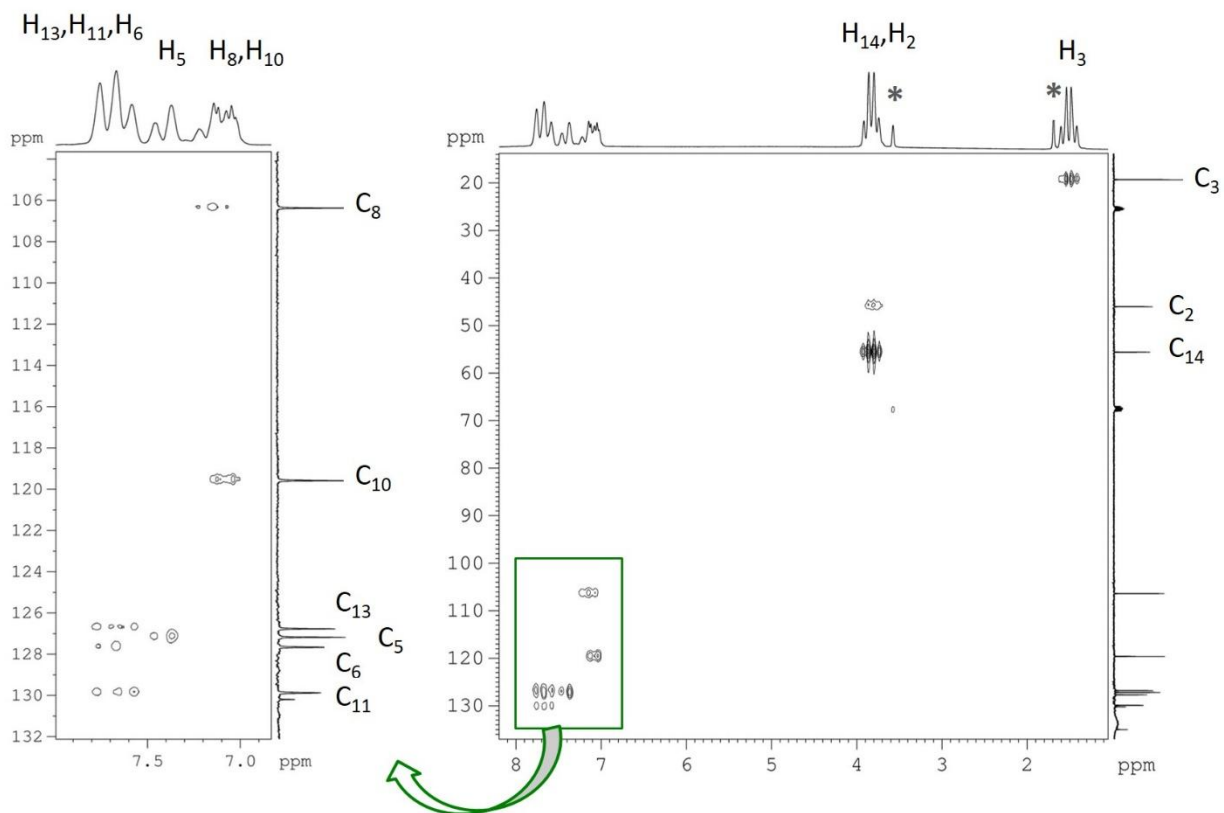


**Figure 3.** 2D  $^{13}\text{C}$ - $^1\text{H}$  HSQC spectrum ( $^1\text{H}$  and  $^{13}\text{C}$  Larmor frequencies 400.13 and 100.61 MHz, respectively) recorded on *S*-naproxen in PBLG/THF- $d_8$  at 300 K using a data matrix of 2048 ( $t_2$ )  $\times$  256 ( $t_1$ ) with 16 scans per  $t_1$  increment. Data were processed using zero-filling up to 512 points in  $t_1$  dimension and a qsrine filter in both dimensions. Solvent peaks are labeled with asterisks.

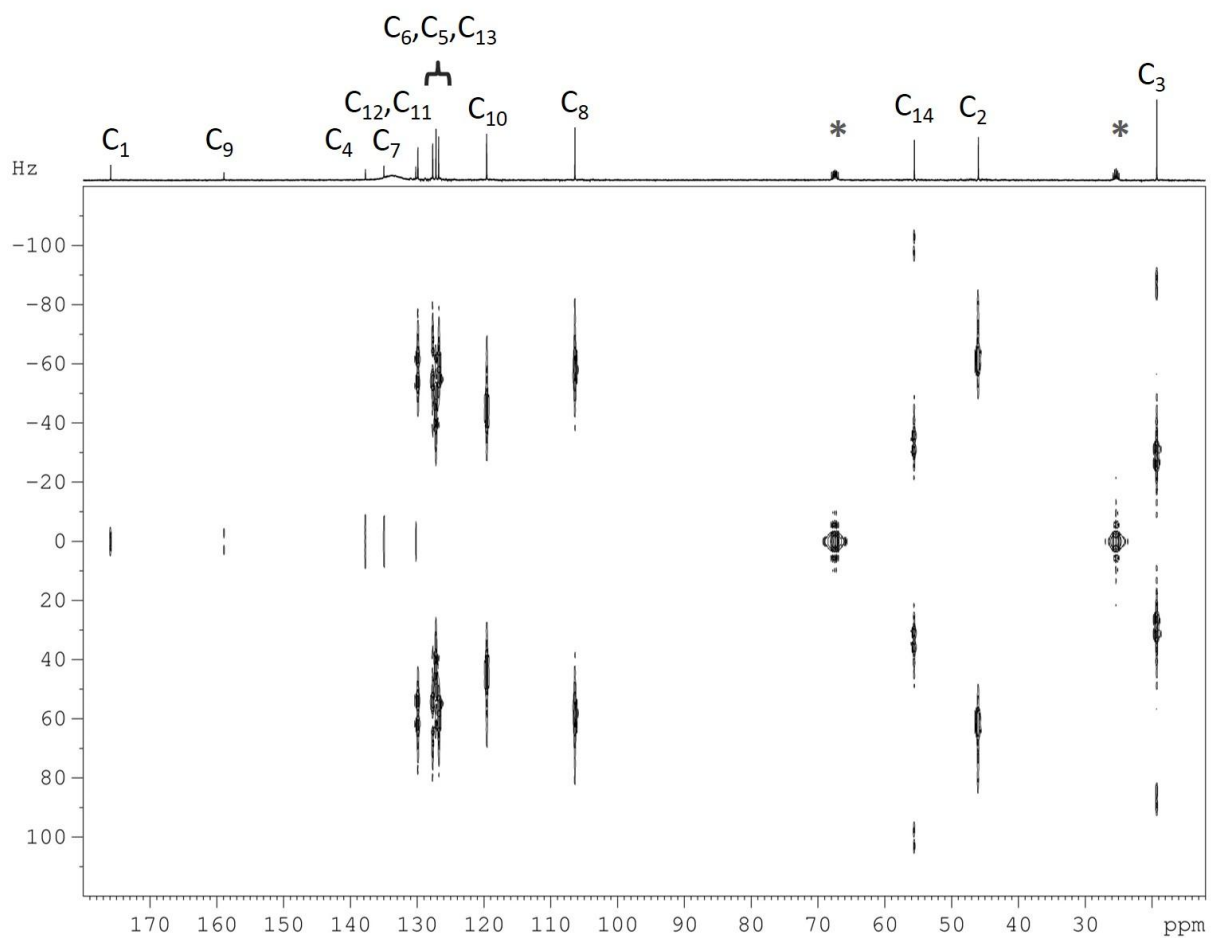


**Figure 4.** 2D  $^{13}\text{C}$ - $^1\text{H}$   $J$ -resolved spectrum ( $^1\text{H}$  and  $^{13}\text{C}$  Larmor frequencies 400.13 and 100.61 MHz, respectively) recorded on *S*-naproxen in PBLG/THF- $d_8$  at 300 K using a data matrix of 2048 ( $t_2$ )  $\times$  128 ( $t_1$ ) with 128 scans per  $t_1$  increment. The relaxation delays were 1 s. Data were processed using zero-filling up to 256 points in  $t_1$  dimension and no filter. Solvent peaks are labeled with asterisks.

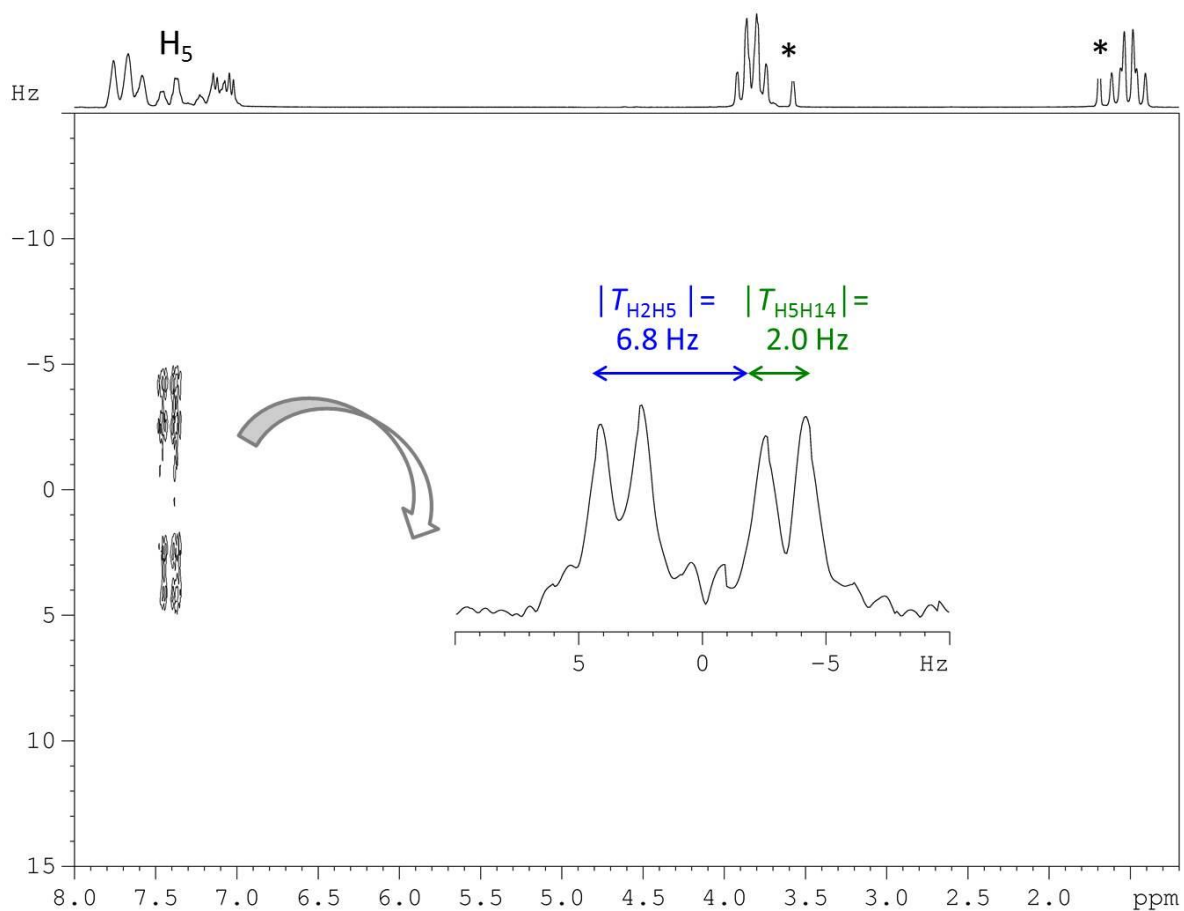


**Figure 5.** 2D  $^1\text{H}$ - $^1\text{H}$  SERF spectrum (Larmor frequency 400.13 MHz) recorded on S-naproxen in PBLG/THF- $d_8$  at 300 K where the offsets of the selective pulses were set at  $\nu_5$  on the F1 channel and at  $\nu_{2,14}$  on the F2 channel. This experiment let the  $\text{H}_2\text{H}_5$  and  $\text{H}_5\text{H}_{14}$  couplings evolve in  $t_1$  so they can be trivially measured on the  $F_1$  dimension. The SERF spectrum was recorded using a data matrix of 2048 ( $t_2$ )  $\times$  400 ( $t_1$ ) with 8 scans per  $t_1$  increment. The relaxation delays were 1 s. Data were processed using zero-filling up to 1024 points and a qsine filter in  $t_1$  dimension. The duration of the RE-BURP refocusing and the E-BURP excitation pulses for  $\text{H}_5$  was 61.9 ms (corresponding to a frequency width of 80 Hz) while the duration of the RE-BURP refocusing pulse for  $\text{H}_2, \text{H}_{14}$  was 14.5 ms (corresponding to a frequency width of 350 Hz). Column extraction is also shown. Solvent peaks are labeled with asterisks.

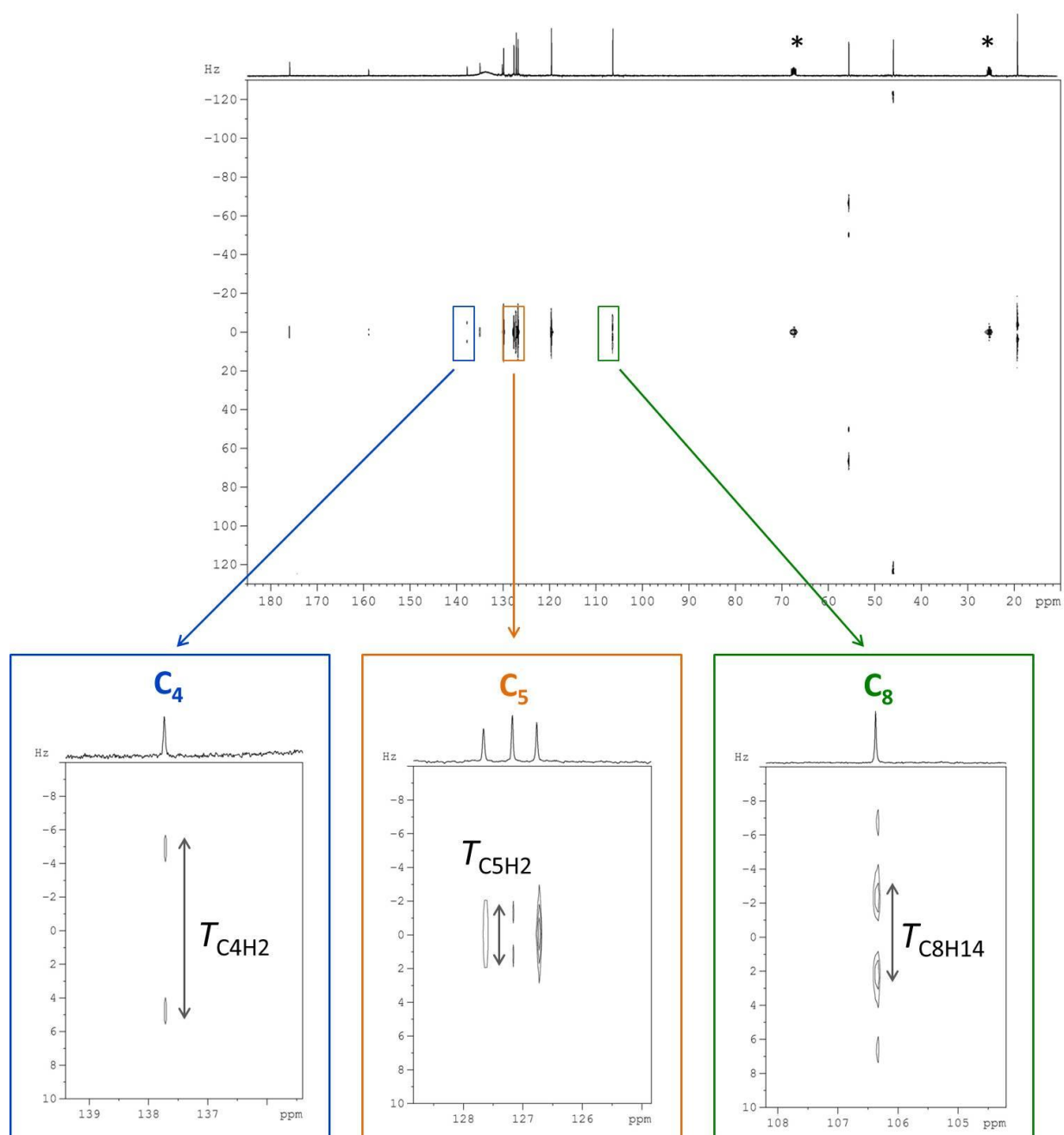


**Figure 6.** 2D  $^{13}\text{C}$ - $^1\text{H}$  HETSERF spectrum ( $^1\text{H}$  and  $^{13}\text{C}$  Larmor frequencies 400.13 and 100.61 MHz, respectively) recorded on S-naproxen in PBLG/THF- $d_8$  at 300 K where the offsets of the  $\pi$  selective pulse on the proton channel was set at  $\nu_{2,14}$ . The spectrum was recorded in 5.5 h using a data matrix of 4096 ( $t_2$ )  $\times$  512 ( $t_1$ ) with 16 scans per  $t_1$  increment. The relaxation delays were 1.5 s. Data were processed using zero-filling up to 1024 points in  $t_1$  dimension and no filter. The duration of the RE-BURP refocusing pulse was 49.5 ms corresponding to a frequency width of 100 Hz. Enlarged maps of selected carbon signals ( $\text{C}_4$ ,  $\text{C}_5$  and  $\text{C}_{13}$ ) are also shown. Solvent peaks are labeled with asterisks.

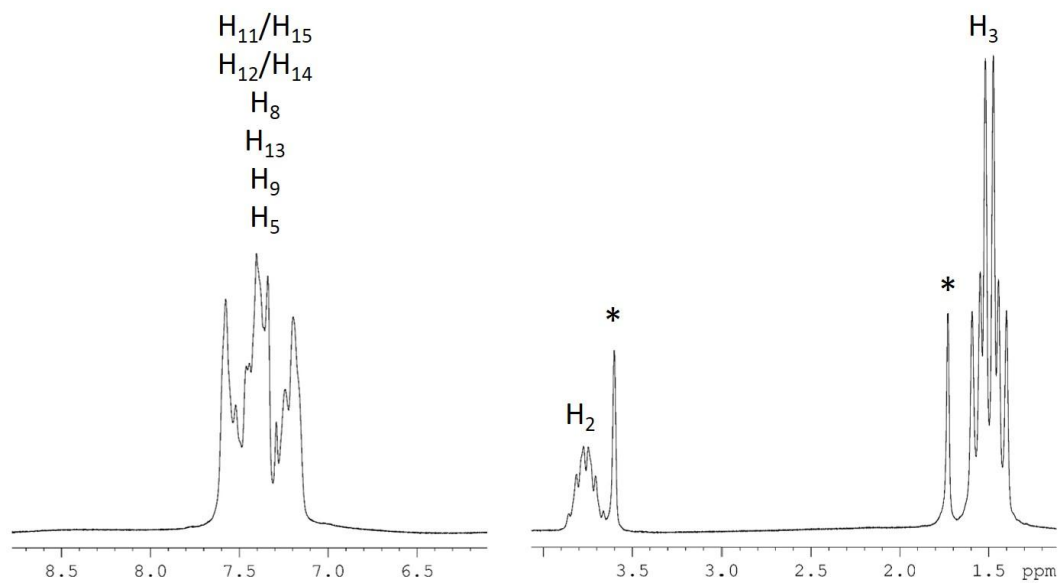


**Figure 7.** 1D  $^1\text{H}$  spectrum (Larmor frequency 500.13 MHz) recorded on *R*-flurbiprofen in PBLG/THF- $\text{d}_8$  at 304 K. Solvent peaks are labeled with asterisks.

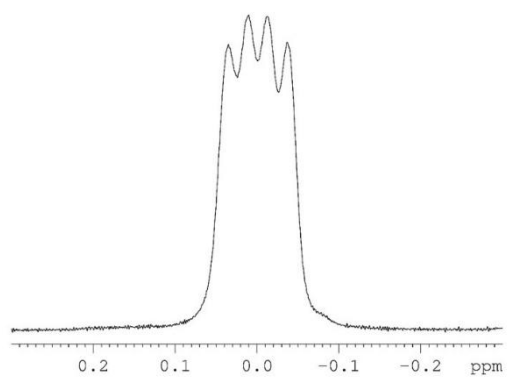


**Figure 8.** 1D  $^{19}\text{F}$  spectrum (Larmor frequency 470.59 MHz) recorded on *R*-flurbiprofen in PBLG/THF- $\text{d}_8$  at 304 K.

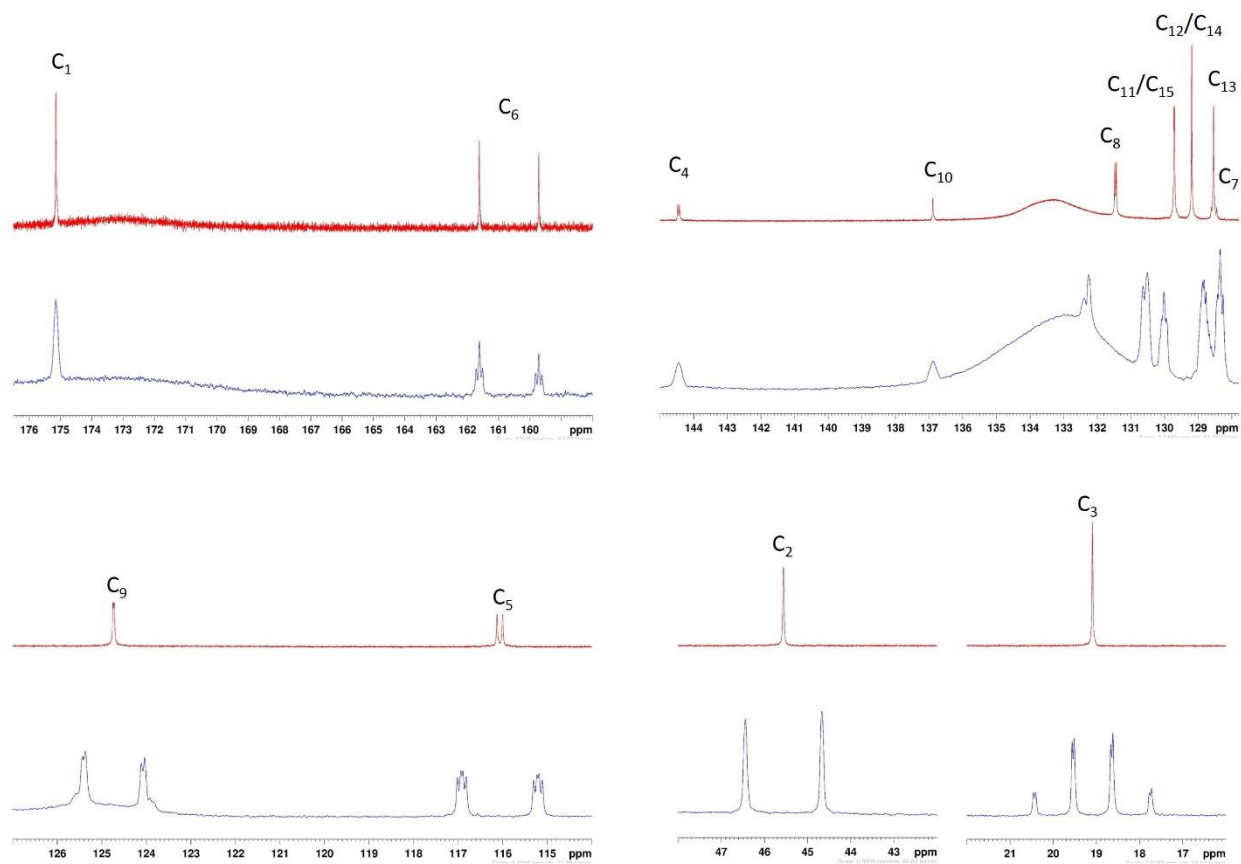


**Figure 9.** 1D  $^1\text{H}$ -coupled (blue) and  $^1\text{H}$ -decoupled (red)  $^{13}\text{C}$  spectra ( $^1\text{H}$  and  $^{13}\text{C}$  Larmor frequencies 500.13 and 125.76 MHz, respectively) recorded on *R*-flurbiprofen in PBLG/THF- $d_8$  at 304 K. The  $^1\text{H}$ -coupled spectrum was recorded by using 65536 points and 14336 scans and processed using an exponential filter (LB = 0.8 Hz). The  $^1\text{H}$ -decoupled spectrum was recorded by using 65536 points and 8192 scans and processed using no filter.

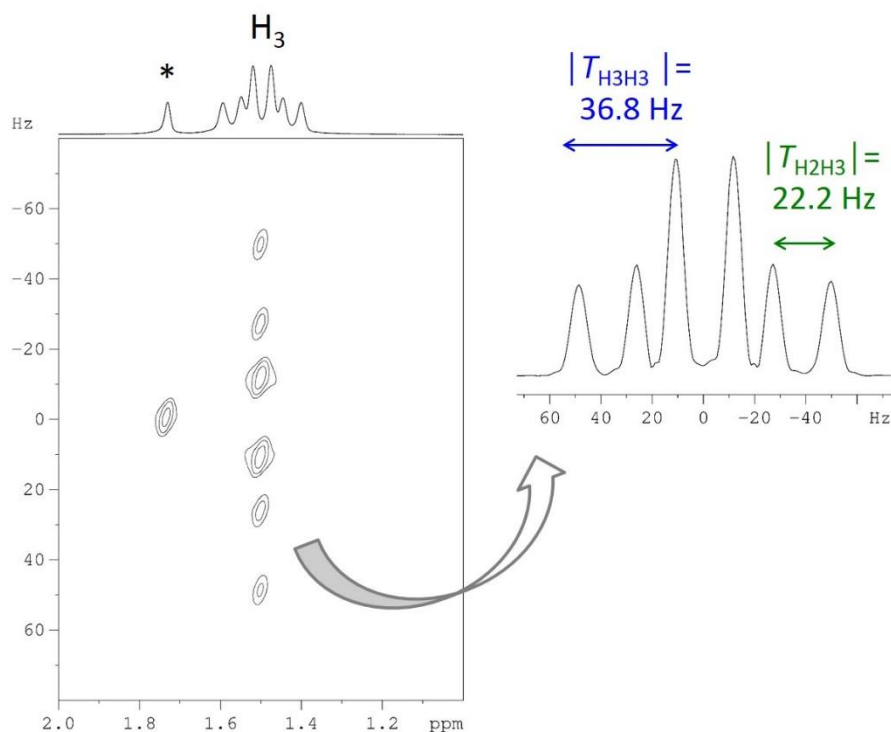


**Figure 10.** 2D  $^1\text{H}$ - $^1\text{H}$  SERF spectrum (Larmor frequency 500.13 MHz) recorded on *R*-flurbiprofen in PBLG/THF- $d_8$  at 304 K where the offset of the excitation selective pulse was set at  $\nu_3$  and the offsets of the refocalisation selective pulse at  $\nu_2$  and at  $\nu_3$ . This experiment let the  $\text{H}_3\text{H}_3$  and  $\text{H}_2\text{H}_3$  couplings evolve in  $t_1$  so they can be trivially measured on the  $F_1$  dimension. The SERF spectrum was recorded in 10 min using a data matrix of 2048 ( $t_2$ )  $\times$  42 ( $t_1$ ) with 4 scans per  $t_1$  increment. The relaxation delays were 1.8 s. Data were processed using zero-filling up to 128 points in  $t_1$  dimension and a sine filter in  $F_1$  dimension. The duration of the RE-BURP refocusing and the E-BURP excitation pulses was 12.4 ms, corresponding to a frequency width of 400 Hz. Solvent peak is labeled with an asterisk.

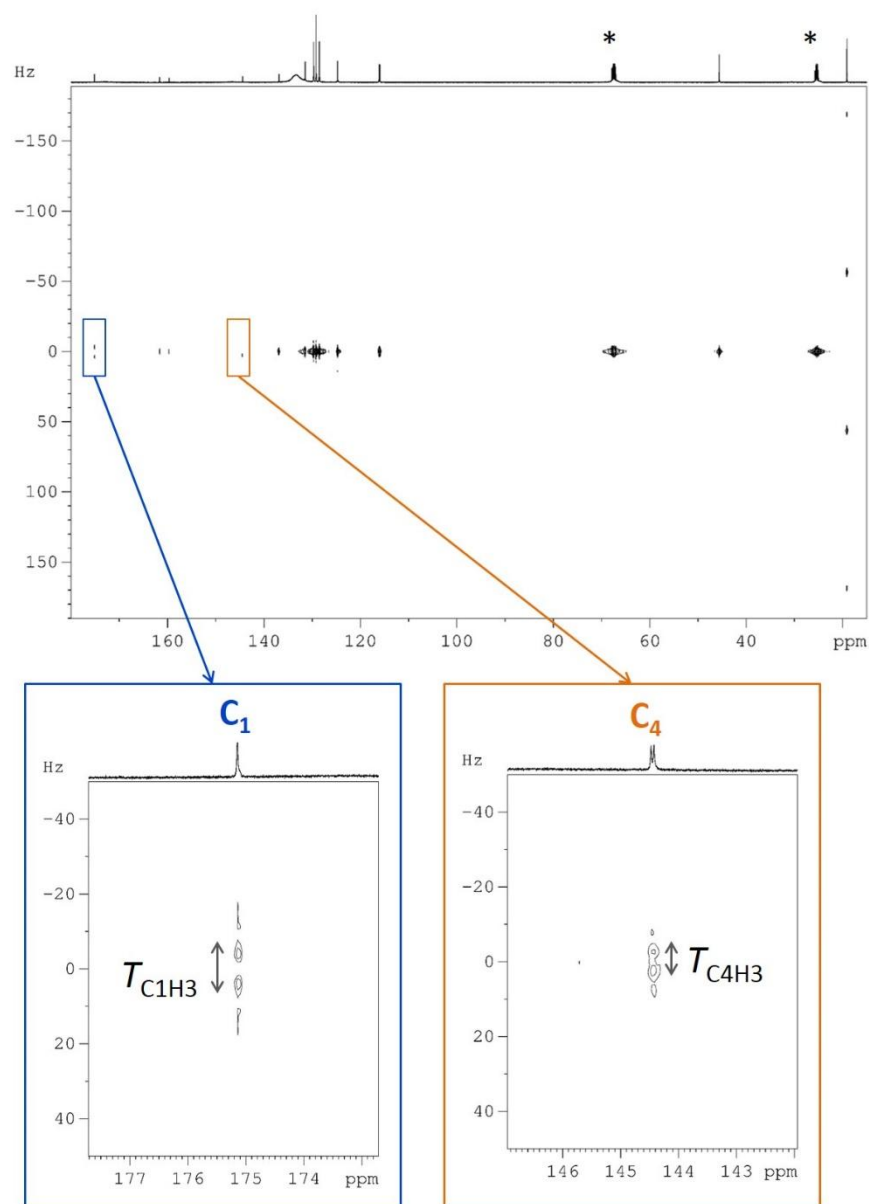


**Figure 11.** 2D  $^{13}\text{C}$ - $^1\text{H}$  HETSERF spectrum ( $^1\text{H}$  and  $^{13}\text{C}$  Larmor frequencies 500.13 and 125.76 MHz, respectively) recorded on *R*-flurbiprofen in PBLG/THF- $d_8$  at 304 K where the offsets of the  $\pi$  selective pulse on the proton channel was set at  $\nu_3$ . The spectrum was recorded in 8.5 h using a data matrix of 4096 ( $t_2$ )  $\times$  200 ( $t_1$ ) with 80 scans per  $t_1$  increment. The relaxation delays were 1.5 s. Data were processed using zero-filling up to 512 points and exponential filter (LB=2.0 Hz) in  $t_1$  dimension. The duration of the RE-BURP refocusing pulse was 12.4 ms corresponding to a frequency width of 400 Hz. Enlarged maps of selected carbon signals ( $C_1$  and  $C_4$ ) are also shown. Solvent peaks are labeled with asterisks.

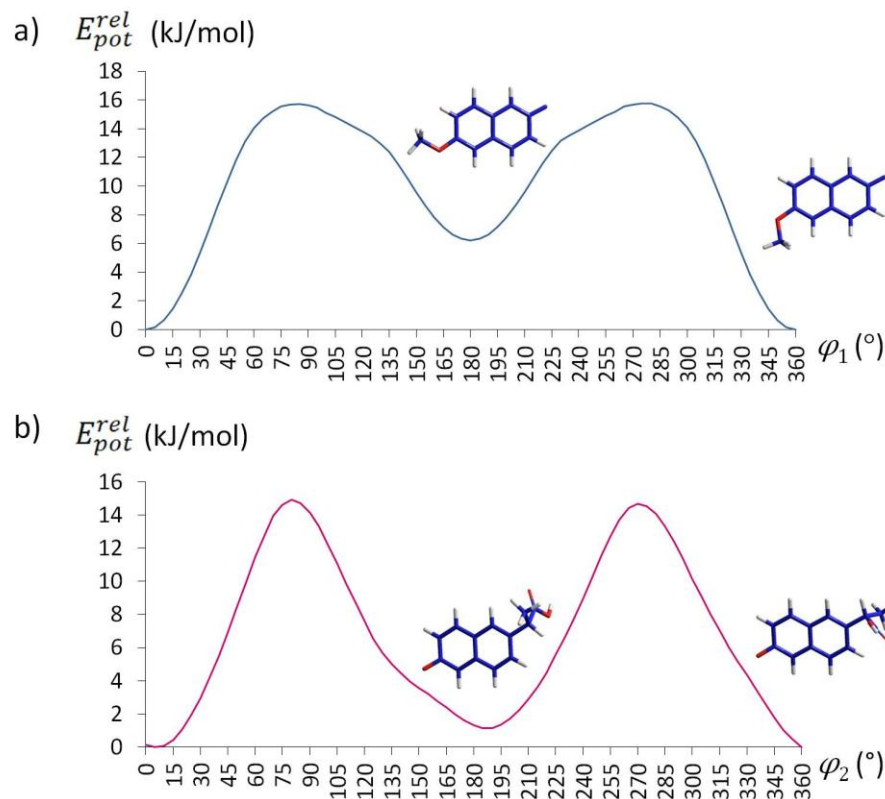


**Figure 12.** Relative potential energy as a function of (a)  $\varphi_1 = \text{C}_8\text{-C}_9\text{-O-C}_{14}$  and (b)  $\varphi_2 = \text{C}_{13}\text{-C}_4\text{-C}_2\text{-H}_2$ , obtained for NAP from relaxed PES calculations at B3LYP/6-31++G\*\* level using Gaussian 03, including structures of the corresponding fragment at the lowest minimum energies. Both curves are obtained by varying the angle over the  $0^\circ - 360^\circ$  range with a  $5^\circ$ -step sampling. The one dimensional scan for  $\varphi_1$  (Figure 1a) reveals two minima, in which the O-C<sub>14</sub> bond of the methoxy group lies preferentially in the plane of the naphthalene ring. The isomer involving the *trans* geometry of the methoxy group ( $\varphi_1 \sim 180^\circ$ ) is about 6 kJ/mol less stable than the *cis* analogue. From the one dimensional scan for  $\varphi_2$  (Figure 1b) two minima are observed, at  $\varphi_2 \sim 5^\circ$  and  $\varphi_2 \sim 185^\circ$ . In this arrangement the  $\alpha$ -hydrogen lies almost in the naphthalene plane and the two bulky methyl and carboxylic acid groups are located on each side of naphthalene plane minimizing the steric repulsion. Thus, the two isomers correspond to a rotation of about  $180^\circ$  of the whole chiral substituent around the C<sub>2</sub>-C<sub>4</sub> bond. Note that, depending on the software and method used for the theoretical calculations, some authors reported additional local minima, including for instance a minimum energy conformer with the C<sub>2</sub>-C<sub>3</sub> bond lying almost in the plane of the naphthalene ring ( $\varphi_2 \sim 135^\circ$ ).<sup>15-35</sup> Despite the potential wells of Figure 1b are not perfectly symmetric, from our calculations at DFT level no real minimum has been observed at  $\varphi_2 \sim 135^\circ$ .

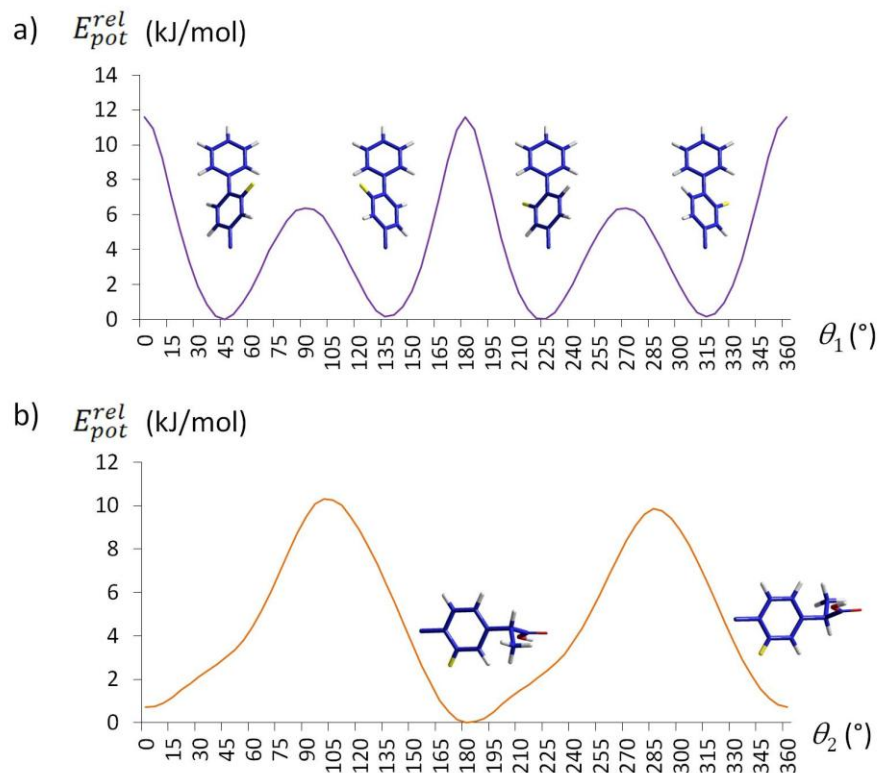
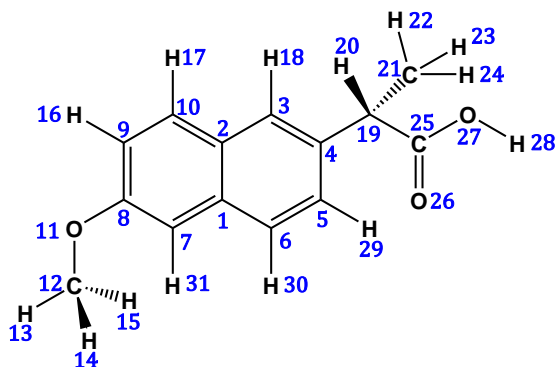


**Figure 13.** Relative potential energy as a function of (a)  $\theta_1 = \text{C}_8\text{-C}_7\text{-C}_{10}\text{-C}_{15}$  and (b)  $\theta_2 = \text{C}_5\text{-C}_4\text{-C}_2\text{-H}_2$  obtained for FLU from relaxed PES calculations at B3LYP/6-31++G\*\* level using Gaussian 03, including structures of the corresponding fragment at the lowest minimum energies. Both curves are obtained by varying the angle over the  $0^\circ - 360^\circ$  range with a  $5^\circ$ -step sampling. From the one dimensional scan for the torsion angle  $\theta_1$  between the two rings (Figure 2a), four minima can be seen, at  $\theta_1 = \pm 45^\circ$  and  $180^\circ \pm 45^\circ$ . As for torsion angle  $\theta_2$  of the chiral substituent around the  $\text{C}_2\text{-C}_4$  axis (Figure 2b) two minima are observed, at  $\theta_2 \sim 5^\circ$  and  $\theta_2 \sim 185^\circ$ . As found for NAP, the steric repulsion due to the two bulky methyl and carboxylic acid groups makes the  $\alpha$ -hydrogen almost coplanar with the fluorinated ring.

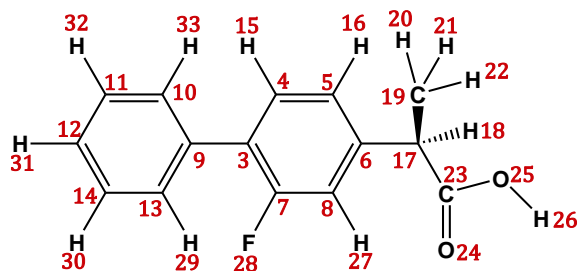
**Table 4.** Averaged geometry obtained by the Gaussian03 software package (B3LYP/6-31++G\*\*) for the four conformers of *S*-naproxen and used in the AP-DPD treatment. Bond lengths  $r_{ij}$  are given in Å; bond angles  $\theta_{ijk}$  and dihedral angles  $\varphi_{ijks}$  are expressed in degrees. The structure gives the numbering of the sites.



$i$	atom type	$j$	$r_{ij}$	$k$	$\theta_{ijk}$	$s$	$\varphi_{ijks}$
1	C						
2	C	1	1.43250				
3	C	2	1.42012	1	119.370		
4	C	3	1.38173	2	121.541	1	
5	C	4	1.42262	3	118.783	2	
6	C	5	1.37730	4	121.119	3	
7	C	1	1.41962	6	122.269	5	180.000
8	C	7	1.38285	1	120.444	6	180.000
9	C	8	1.42210	7	120.233	1	0.000
10	C	9	1.37618	8	120.072	7	0.000
11	O	8	1.36740	7	125.762	1	-179.965
12	C	11	1.42215	8	118.732	7	$\varphi_1$
13	H	12	1.09507	11	109.532	8	179.860
14	H	12	1.09507	11	109.532	8	298.569
15	H	12	1.09507	11	109.532	8	61.149
16	H	9	1.08422	8	120.072	7	180.000
17	H	10	1.08690	9	119.710	8	180.000
18	H	3	1.08765	2	118.472	10	0.000
19	C	4	1.52890	3	121.034	2	180.000
20	H	19	1.09442	4	107.579	3	$\varphi_2$
21	C	19	1.53868	4	112.620	20	-120.742
22	H	21	1.09365	19	110.521	4	56.790
23	H	21	1.09365	19	110.521	4	176.799

24	H	21	1.09365	19	110.521	4	-63.282
25	C	19	1.52317	4	109.389	20	115.780
26	O	25	1.21400	19	125.779	4	91.293
27	O	25	1.35682	19	112.026	4	-87.619
28	H	27	0.97262	25	107.084	19	177.136
29	H	5	1.08658	6	119.663	1	180.000
30	H	6	1.08695	1	118.946	7	0.000
31	H	7	1.08488	8	120.203	9	180.000

**Table 5.** Averaged geometry obtained by the Gaussian03 software package (B3LYP/6-31++G\*\*) for the eight conformers of *R*-flurbiprofen and used in the AP-DPD treatment. Bond lengths  $r_{ij}$  are given in Å; bond angles  $\theta_{ijk}$  and dihedral angles  $\varphi_{ijkl}$  are expressed in degrees. The structure gives the numbering of the sites.



$i$	atom type	$j$	$r_{ij}$	$k$	$\theta_{ijk}$	$s$	$\varphi_{ijkl}$
1	X						
2	X	1	1.00000				
3	C	2	0.74315	1	90.000		
4	C	3	1.40058	2	123.348	1	0.000
5	C	4	1.38820	3	123.661	2	180.000
6	C	5	1.40008	4	119.768	3	0.000
7	C	3	1.40705	4	115.422	5	0.000
8	C	7	1.39365	3	122.200	4	0.000
9	C	2	0.74315	1	90.000	3	180.000
10	C	9	1.40605	3	120.801	4	45.000
11	O	10	1.39562	9	120.785	3	180.000
12	C	11	1.39736	10	120.277	9	0.000

13	C	9	1.40605	10	118.358	11	0.000
14	C	13	1.39562	9	120.785	10	0.000
15	H	4	1.08570	5	119.309	6	180.000
16	H	5	1.08545	6	119.875	8	180.000
17	C	6	1.52725	8	120.613	7	180.000
18	H	17	1.09300	6	107.589	8	0.000
19	C	17	1.54220	6	109.936	18	122.755
20	H	19	1.09360	17	110.918	6	-179.288
21	H	19	1.09360	17	110.618	6	-58.808
22	H	19	1.09360	17	110.618	6	60.623
23	C	17	1.52550	6	110.542	18	-113.161
24	O	23	1.21243	17	124.914	6	101.581
25	O	23	1.35835	17	112.931	6	-78.167
26	H	25	0.97240	23	107.018	17	178.285
27	H	8	1.08482	6	121.610	5	180.000
28	F	7	1.36193	8	116.990	6	180.000
29	H	13	1.08535	14	119.619	12	180.000
30	H	14	1.08626	12	120.126	11	180.000
31	H	12	1.08610	11	120.254	10	180.000
32	H	11	1.08626	12	120.126	14	180.000
33	H	10	1.08535	11	119.619	12	180.000

**Table 6.** Optimised values of the iteration parameters used in the conformational analysis with the AP-DPD approach of the NAP molecule dissolved in PBLG/THF-d<sub>8</sub>.

	NAP in PBLG/THF-d <sub>8</sub>
$\varphi_1^{max}$ (degree)	0 ± 10
$\varphi_2^{max}$ (degree)	16 ± 6
$A_{\varphi_1}$	0.87 ± 0.02
$A_{\varphi_2}$	0.66 ± 0.03
$h_{\varphi_1}$ (degree)	12.0 <sup>[a]</sup>
$h_{\varphi_2}$ (degree)	17.0 <sup>[a]</sup>
$\varepsilon_{C_6,C_{13}}$ (RT)	-0.0096 ± 0.0003
$\varepsilon_{C_5,C_7}$ (RT)	-0.0045 ± 0.0003
$\varepsilon_{C_9,O} = \varepsilon_{C_4,C_2}$ (RT)	0.0059 ± 0.0002
$\varepsilon_{C_2,H_2}$ (RT)	-0.0123 ± 0.0003
$\varepsilon_{C_2,C_3}$ (RT)	-0.0076 ± 0.0006
$\varepsilon_{H_2,C_3}$ (RT)	0.0054 ± 0.0006
$\varepsilon_{O,C_{14}}$ (RT)	0.0073 ± 0.0003
RMS (Hz)	0.40

<sup>[a]</sup> after parameterization.

**Table 7.** Optimised values of the iteration parameters used in the conformational analysis with the AP-DPD approach of the FLU molecule dissolved in PBLG/THF-d<sub>8</sub>.

	FLU in PBLG/THF-d <sub>8</sub>
$\theta_1^{max}$ (degree)	43.9 ± 0.7
$\theta_2^{max}$ (degree)	8 ± 2
$A_{\theta_2}$	0.43 ± 0.02
$h_{\theta_1}$ (degree)	13.5 ± 1.0
$h_{\theta_2}$ (degree)	15.9 ± 1.2
$\varepsilon_{C_4,C_7} = \varepsilon_{C_{10},C_{13}}$ (RT)	0.00009 ± 0.00003
$\varepsilon_{C_6,C_8}$ (RT)	-0.0005 ± 0.0003
$\varepsilon_{C_{11},C_{15}}$ (RT)	-0.0070 ± 0.0002
$\varepsilon_{C_6,F_6}$ (RT)	0.00297 ± 0.00006
$\varepsilon_{C_2,H_2}$ (RT)	-0.0097 ± 0.0002
$\varepsilon_{C_2,C_3}$ (RT)	-0.0048 ± 0.0006
$\varepsilon_{H_2,C_3}$ (RT)	0.0009 ± 0.0008
RMS (Hz)	0.34

## References

- 1S E. Bednarek, W. Bocian, J. Cz. Dobrowolski, L. Kozerski, N. Sadlej-Sosnowska, J. Sitkowski, *J. Mol. Struct.*, 2001, **559**, 369.
- 2S F. Lahmani, K. Le Barbu-Debus, N. Seurre, A. Zehnacker-Rentien, *Chem. Phys. Lett.*, 2003, **375**, 636.
- 3S L. Alvarez-Valtierra, J. W. Young, D. W. Pratt, *Chem. Phys. Lett.*, 2011, **509**, 96.